Combined Experimental and Computational Investigation of the Mechanism of Nickel-Catalyzed Three-Component Addition Processes

Hrant P. Hratchian,† Sanjoy K. Chowdhury, Víctor M. Gutiérrez-García, Kande K. D. Amarasinghe, Mary Jane Heeg,‡ H. Bernhard Schlegel,*,† and John Montgomery*

Department of Chemistry, Wayne State University, Detroit, Michigan 48202-3489

Received July 14, 2004

The mechanism of nickel-catalyzed couplings of an enone, alkyne, and organozinc has been studied. Adducts of the substrates with nickel(0) have been isolated and characterized, and their reactivity was examined. A potential intermediate was demonstrated to not be kinetically competent in catalytic cyclizations. A computational approach employing the B3LYP density functional method and the 6-31G(d) basis set was used to examine mechanistic possibilities that were consistent with experimental observations, and a modified mechanism for the catalytic cyclizations was formulated. The newly proposed mechanism involves production of an active catalyst that involves a novel interaction between Ni(0) and dimethylzinc.

Introduction

Nickel metallacycles have been known for decades, and their methods of preparation include oxidative cyclization of two π components,[1] oxidative addition into the σ bond of a cyclic precursor,[2] addition of a bis-metalated precursor to a nickel dihalide,[3] and ortho metalation.[4] The route involving oxidative cyclization of two π components is of particular synthetic significance, since the formation of metallacycles by such a sequence is believed to be a critical mechanistic step in a number of important catalytic processes. For instance, the dimerization and oligomerization of butadienes,[1a,5] the [4 + 2] cycloaddition of alkynes and dienes,[6] and the cyclotrimerization of alkynes[7] are extensively studied processes that involve metallacycles formed by the oxidative cyclization mechanism.

In studies from our own laboratories and others, a number of nickel-catalyzed processes have been studied that involve three-component couplings of two π components with a main-group organometallic.[1c,8] Whereas a number of mechanisms have been considered for the different variants studied, a metallacycle-based mechanism is consistent with most of the experimental observations that have resulted from this program (Scheme 1). The formation of the bis-π-complex **1**,

* To whom correspondence should be addressed. E-mail: hbs@chem.wayne.edu (H.B.S.); jwm@chem.wayne.edu (J.M.).

† Institute for Scientific Computing, Wayne State University.

‡ To whom correspondence regarding X-ray crystallographic determinations should be directed.

(1) (a) Wilke, G. *Angew. Chem., Int. Ed. Engl.* **1988**, *27*, 185. (b) Smith, A. K. In *Comprehensive Organometallic Chemistry II*; Puddephatt, R. J., Ed.; Pergamon Press: New York, 1995; Vol. 9, p 29. (c) Montgomery, J. Organometallic Complexes of Nickel. In *Science of Synthesis*; Trost, B. M., Lautens, M., Eds.; Thieme: Stuttgart, Germany, 2001; Vol. 1, pp 11−62. (d) Kaschube, W.; Schröder, W.; Pörschke, K. R.; Angermund, K.; Krüger, C. *J. Organomet. Chem.* **1990**, *389*, 399. (e) Grubbs, R. H.; Miyashita, A. *J. Am. Chem. Soc.* **1978**, *100*, 1300. (f) McKinney, R. J.; Thorn, D. L.; Hoffman, R.; Stockis, A. *J. Am. Chem. Soc.* **1981**, *103*, 2595. (g) Büch, H. M.; Binger, P.; Benn, R.; Rufinska, A. *Organometallics* **1987**, *6*, 1130. (h) Koo, K.; Hillhouse, G. L. *Organometallics* **1998**, *17*, 2924. (i) Maekawa, M.; Munakata, M.; Kuroda-Sowa, T.; Hachiya, K. *Inorg. Chim. Acta* **1995**, *230*, 249.

(2) (a) Echavarren, A. M.; Castaño, A. M. *Advances in Metal-Organic Chemistry*; Liebeskind, L. S., Ed.; JAI Press: London, 1998; Vol. 6, p 1. (b) Bercot, E. A.; Rovis, T. *J. Am. Chem. Soc.* **2002**, *124*, 174. (c) Deming, T. J. *J. Am. Chem. Soc.* **1998**, *120*, 4240. (d) Deming, T. J.; Curtin, S. A. *J. Am. Chem. Soc.* **2000**, *122*, 5710.

(3) (a) Grubbs, R. H.; Miyashita, A.; Liu, M.; Burk, P. L. *J. Am. Chem. Soc.* **1977**, *99*, 3863. (b) Grubbs, R. H.; Miyashita, A.; Liu, M.; Burk, P. L. *J. Am. Chem. Soc.* **1978**, *100*, 2418.

(4) Carmona, E.; Gutiérrez-Puebla, E.; Marín, J. M.; Monge, A.; Paneque, M.; Poveda, M. L.; Ruiz, C. *J. Am. Chem. Soc.* **1989**, *111*, 2883.

(5) (a) Benn, R.; Büssemeier, B.; Holle, S.; Jolly, P. W.; Mynott, R.; Tkatchenko, I.; Wilke, G. *J. Organomet. Chem.* **1985**, *279*, 63. (b) Keim, W. *Angew. Chem., Int. Ed. Engl.* **1990**, *29*, 235. (c) Wender, P. A.; Ihle, N. C. *Tetrahedron Lett.* **1987**, *28*, 2451. (d) Wender, P. A.; Snapper, M. L. *Tetrahedron Lett.* **1987**, *28*, 2221. (e) Wender, P. A.; Ihle, N. C.; Correia, C. R. D. *J. Am. Chem. Soc.* **1988**, *110*, 5904. (f) Wender, P. A.; Tebbe, M. J. *Synthesis* **1991**, 1089. (g) Wender, P. A.; Nuss, J. M.; Smith, D. B.; Suárez-Sobrino, A.; Vagberg, J.; Decosta, D.; Bordner, J. *J. Org. Chem.* **1997**, *62*, 4908. (h) Wender, P. A.; Ihle, N. C. *J. Am. Chem. Soc.* **1986**, *108*, 4678.

(6) (a) Wender, P. A.; Jenkins, T. E. *J. Am. Chem. Soc.* **1989**, *111*, 6432. (b) Wender, P. A.; Smith, T. E. *J. Org. Chem.* **1995**, *60*, 2962. (c) Wender, P. A.; Jenkins, T. E.; Suzuki, S. *J. Am. Chem. Soc.* **1995**, *117*, 1843. (d) Wender, P. A.; Smith, T. E. *J. Org. Chem.* **1996**, *61*, 824. (e) Wender, P. A.; Smith, T. E. *Tetrahedron* **1998**, *54*, 1255.

(7) (a) Reppe, W.; Schlichting, O.; Klager, K.; Toepel, T. *Justus Liebigs Ann. Chem.* **1948**, *560*, 1. (b) Lautens, M.; Klute, W.; Tam, W. *Chem. Rev.* **1996**, *96*, 49. (c) Bhatarah, P.; Smith, E. H. *J. Chem. Soc., Perkin Trans. 1* **1992**, 2163. (d) Sato, Y.; Nishimata, T.; Mori, M. *J. Org. Chem.* **1994**, *59*, 6133. (e) Ikeda, S.; Watanabe, H.; Sato, Y. *J. Org. Chem.* **1998**, *63*, 7026. (f) Shanmugasundaram, M.; Wu, M. S.; Jeganmohan, M.; Huang, C.-W.; Cheng, C.-H. *J. Org. Chem.* **2002**, *67*, 7724. See also: (g) Louie, J.; Gibby, J. E.; Farnworth, M. V.; Tekavec, T. N. *J. Am. Chem. Soc.* **2002**, *124*, 15188.

(8) For representative examples, see: (a) Montgomery, J. *Acc. Chem. Res.* **2000**, *33*, 467. (b) Ikeda, S. *Acc. Chem. Res.* **2000**, *33*, 511. (c) Sato, Y.; Takimoto, M.; Mori, M. *J. Am. Chem. Soc.* **2000**, *122*, 1624. (d) Kimura, M.; Ezoe, A.; Shibata, K.; Tamaru, Y. *J. Am. Chem. Soc.* **1998**, *120*, 4033. (e) Kimura, M.; Fujimatsu, H.; Ezoe, A.; Shibata, K.; Shimizu, M.; Matsumoto, S.; Tamaru, Y. *Angew. Chem., Int. Ed.* **1999**, *38*, 397. (f) Ezoe, A.; Kimura, M.; Inoue, T.; Mori, M.; Tamaru, Y. *Angew. Chem., Int. Ed.* **2002**, *41*, 2784. (g) Miller, K. M.; Huang, W.-S.; Jamison, T. F. *J. Am. Chem. Soc.* **2003**, *125*, 3442. (h) Patel, S. J.; Jamison, T. F. *Angew. Chem., Int. Ed.* **2003**, *42*, 1364. (i) Montgomery, J. *Angew. Chem., Int. Ed.* **2004**, *43*, 3890.

10.1021/om049471a CCC: $27.50
Publication on Web 09/02/2004

Scheme 1

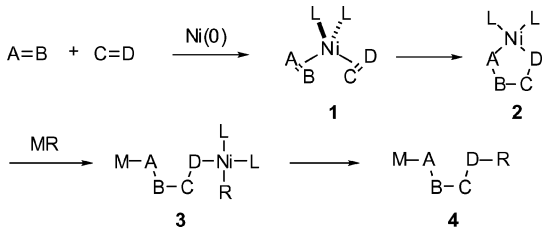

followed by oxidative cyclization, would afford metallacycle **2**. Transmetalation of the main-group organometallic to **2** would afford intermediate **3**, and reductive elimination of this structure would afford the observed three-component coupling product **4**. The π components that participate in processes of this type include enones, unsaturated acyloxazolidinones, nitroalkenes, alkylidene malonates, alkynes, dienes, allenes, aldehydes, and ketones. The organometallics that have been employed in various applications include organozincs, organoaluminums, organoboranes, alkenylzirconiums, and acetylenic tins, as well as metal hydrides of silicon and aluminum. Given the considerable attention that has recently been devoted to this class of reactions, we have attempted to provide insight into the mechanism of these processes by a combined experimental and theoretical approach. In this work, we have isolated, characterized, and examined the reactivity of several organometallic species that may be involved in the processes, and we have carried out an initial investigation of asymmetric processes utilizing a ligand class that is analogous to those that provide well-behaved nickel complexes. We have used these experimental observations about structure and reactivity as a starting point for a hybrid density functional theory study of the reaction mechanism of the three-component nickel-catalyzed addition of an enone, alkyne, and organozinc. The combination of these approaches allows us to evaluate the previously proposed mechanism for this reaction class and to propose a modified description. This interactive and collaborative use of experiment and theory allows a detailed analysis of mechanistic issues that could not be resolved by either individual approach.

Structural Studies

Whereas many variants of three-component nickel-catalyzed couplings have been developed, we viewed the addition of an enone, alkyne, and organozinc (i.e. generation of products **7** and **8**) as a particularly relevant place to begin our studies (Scheme 2). Not only had the synthetic utility of the process been well studied by Ikeda and by us, but the metallacycle derived from oxidative cyclization of an enone and alkyne had also been proposed as a key common intermediate in a very diverse range of synthetic procedures.[8a,b,9] For instance, in addition to the production of compounds **7** and **8** in organozinc-mediated cyclizations, additional reactivity manifolds, including [2 + 2 + 2] cycloadditions (products **9** and **10**), [3 + 2] alkylative cycloadditions (product **11**), and [2 + 1] oxidative cycloadditions (product **12**) had been demonstrated in processes that likely involved the intermediacy of metallacycle **6**. Therefore, we envisioned that some knowledge of the precise structural interactions between a Ni(0) catalyst and the organic substrates of interest could provide a very useful starting point for additional study.

Scheme 2

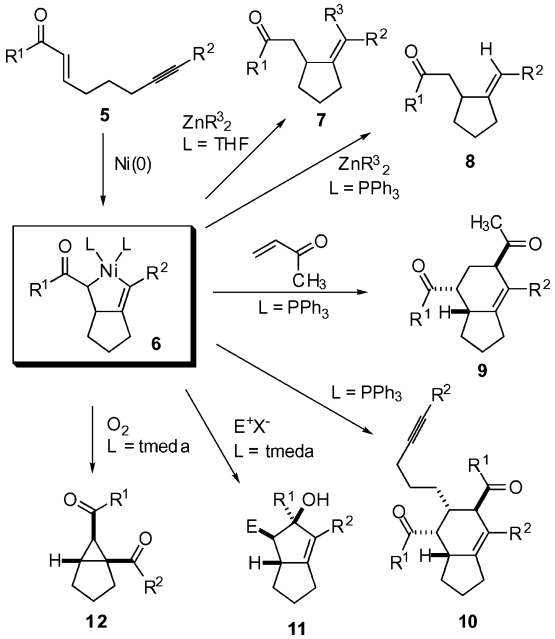

Scheme 3

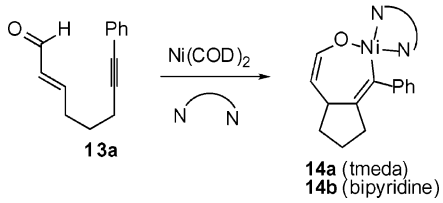

With this goal in mind, alkynyl enal **13a** was treated with a stoichiometric quantity of $Ni(COD)_2$ and tmeda (Scheme 3, Figure 1).[9a] A deep red solution resulted, and upon concentration, filtration, and recrystallization with hexane/THF, a red crystalline solid was obtained. Single-crystal X-ray analysis of the crystalline solid **14a** was carried out, and the molecular structure is the η^1 O-bound tautomer of the metallacycle proposed in catalytic cyclizations. A square-planar geometry is observed, and the Ni−O−C bond angle of 125° clearly demonstrates the η^1 nature of the enolate. The metallacycle was further characterized by IR, ^{1}H and ^{13}C NMR, and elemental analysis, and NMR assignments were rigorously made utilizing 2D techniques. The η^1 O-bound solution structure was confirmed by the spectroscopic data. The O-bound structure is unusual, since most classes of late-metal enolates exist as the C-bound tautomer. The extensive studies from Bergman and Heathcock with a variety of mid- and late-metal enolates clearly document this trend, and enolates of nickel were reported in their study to be η^1 C-bound.[10] Significantly,

(9) (a) Amarasinghe, K. K. D.; Chowdhury, S. K.; Heeg, M. J.; Montgomery, J. *Organometallics* **2001**, *20*, 370. (b) Chowdhury, S. K.; Amarasinghe, K. K. D.; Heeg, M. J.; Montgomery, J. *J. Am. Chem. Soc.* **2000**, *122*, 6775. (c) Seo, J.; Chui, H. M. P.; Heeg, M. J.; Montgomery, J. *J. Am. Chem. Soc.* **1999**, *121*, 476. (d) Mahandru, G. M.; Skauge, A. R. L.; Chowdhury, S. K.; Amarasinghe, K. K. D.; Heeg, M. J.; Montgomery, J. *J. Am. Chem. Soc.* **2003**, *125*, 13481. (e) Ikeda, S.; Kondo, K.; Sato, Y. *J. Org. Chem.* **1996**, *61*, 8248. (f) Rayabarapu, D. K.; Sambaiah, T.; Cheng, C.-H. *Angew. Chem., Int. Ed.* **2001**, *40*, 1286. (g) Rayabarapu, D. K.; Cheng, C.-H. *Chem. Eur. J.* **2003**, *9*, 3164.

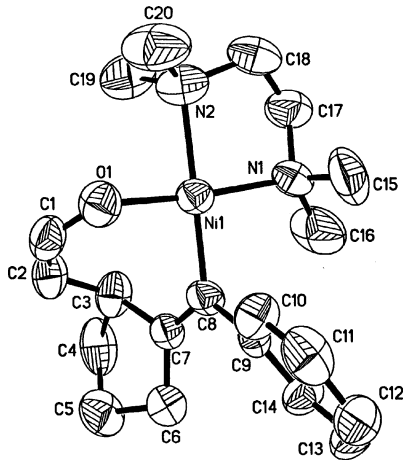

Figure 1. X-ray crystal structure of metallacycle **14a**. Selected bond lengths (Å) and angles (deg): Ni−O = 1.852(6), O−C1 = 1.316(10), C1−C2 = 1.298(11), C2−C3 = 1.508(11), C7−C8 = 1.357(10) C8−Ni = 1.897(7); O−Ni−C8 = 91.3(3), O−Ni−N2 = 88.9(3), N2−Ni−N1 = 85.6(3), N1−Ni−C8 = 94.3(3), Ni−O−C1 = 124.7(5), O−C1−C2 = 132.1(8), C1−C2−C3 = 126.0(8).

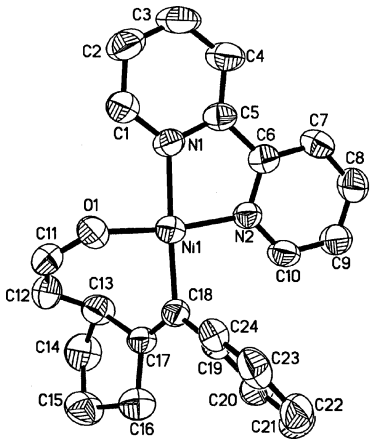

Figure 2. X-ray crystal structure of metallacycle **14b**. Selected bond lengths (Å) and angles (deg): Ni−O = 1.8347(17), O−C11 = 1.319(3), C11−C12 = 1.324(4), C12−C13 = 1.493(4), C17−C18 = 1.333(3), C18−Ni = 1.897(2); O−Ni−C18 = 92.13(8), O−Ni−N1 = 89.62(8), N1−Ni−N2 = 82.35(9), N2−Ni−C18 = 95.87(9), Ni−O−C11 = 127.5(2), O−C11−C12 = 130.6(3), C11−C12−C13 = 125.8(3).

in the NMR spectra of nickel *C*-enolates, the carbon and protons α to the carbonyl appeared at δ −8.0 to 13.6 (^{13}C) and δ 0.75 to 1.88 (^{1}H) compared with the analogous signals for complex **14a**, which appeared at δ 101 (^{13}C) and δ 3.5 (^{1}H). The corresponding bipyridine complex **14b** was also prepared, and its structural and spectroscopic properties were directly analogous to those of complex **14a** (Scheme 3, Figure 2).

The isolation of complexes **14a** and **14b** provides structural details about the metallacycle derived from oxidative cyclization of an enone and alkyne, but the features of the starting bis π complex itself (prior to oxidative cyclization) must also be considered in formulating a complete picture of the overall transformation. Therefore, we were very pleased to observe that bis-enones, which were also utilized in catalytic cyclizations

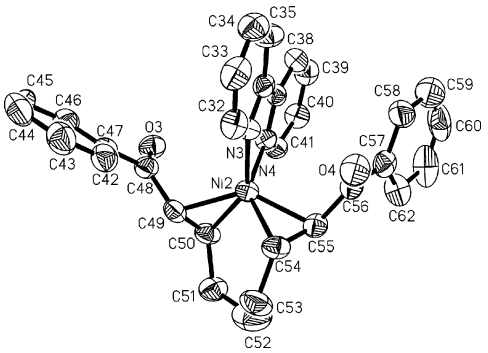

Figure 3. X-ray crystal structure of complex **16**. Selected bond lengths (Å) and angles (deg): Ni−C49 = 2.015(6), Ni−C50 = 2.004(6), Ni−C54 = 2.017(6), Ni−C55 = 2.051(7); C50−Ni−C54 = 97.6(3).

Scheme 4

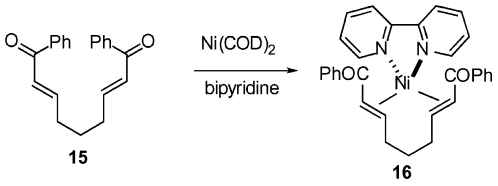

Scheme 5

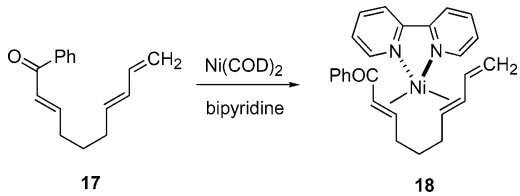

developed by our group,[11] could be converted into isolable Ni(0) π complexes (Scheme 4, Figure 3). Under the same conditions that resulted in the formation of the metallacycles from alkynyl enals described above, treatment of bis-enone **15** with stoichiometric quantities of Ni(COD)$_2$ and bipyridine resulted in the formation of complex **16**. Although the substrate structure varies (bis-enone vs alkynyl enal), it is noteworthy that the ligand systems are identical within the two classes of structures.

Dienes are yet another type of unsaturated subunit that has been utilized in many classes of nickel-catalyzed reactions;[6,8c−f] thus, we were interested in probing the structure of Ni(0) diene complexes within the same series of well-defined compounds described above. Treatment of enone diene **17** with Ni(COD)$_2$ and bipyridine afforded Ni(0) adduct **18** (Scheme 5, Figure 4). As observed with bis-enones, the simple tetrahedral Ni(0) bis π complex was observed. Compound **18** proved to be very unstable, and bulk material was not obtained in satisfactory purity to allow spectroscopic characterization.

Reactivity Studies

With considerable information in hand about structure, we next examined the reactivity of metallacycle **14a**, derived from oxidative cyclization of enal-alkyne

(10) (a) Burkhardt, E. R.; Bergman, R. G.; Heathcock, C. H. *Organometallics* **1990**, *9*, 30. (b) See ref 9d for additional discussion of nickel enolates.

(11) (a) Savchenko, A. V.; Montgomery, J. *J. Org. Chem.* **1996**, *61*, 1562**.** (b) Montgomery, J.; Oblinger, E.; Savchenko, A. V. *J. Am. Chem. Soc.* **1997**, *119*, 4911.

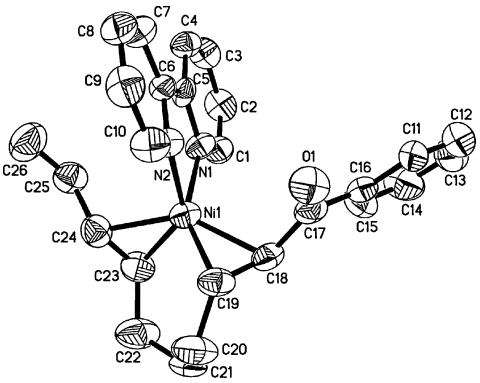

Figure 4. X-ray crystal structure of complex **18**. Selected bond lengths (Å) and angles (deg): Ni−C18 = 2.052(6), Ni−C19 = 1.977(5), Ni−C23 = 2.016(6), Ni−C24 = 2.063(6); C19−Ni−C23 = 97.7(3).

Scheme 6

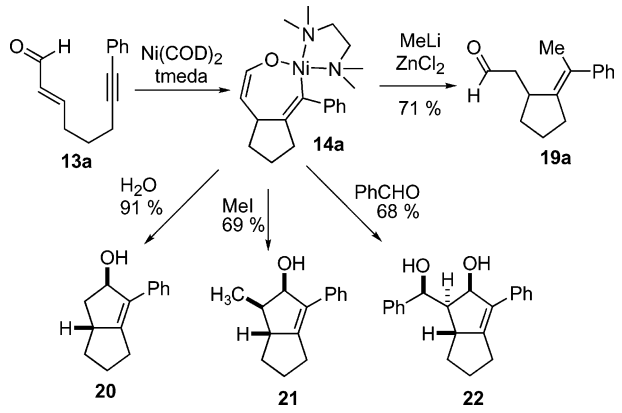

substrate **13a**. Complex **14a** was observed to demonstrate reactivity that closely parallels the nickel-catalyzed chemistry of alkynyl enal **13a**. For instance, treatment of complex **14a** with dimethylzinc (generated in situ from MeLi and $ZnCl_2$) affords a 71% isolated yield of aldehyde **19a**, in direct analogy to the catalytic alkynyl enone/organozinc couplings that we extensively developed (Scheme 6). In addition, the stoichiometric conversion of **14a** to **20**−**22** via nickel enolate protonation with water or alkylation with either methyl iodide or benzaldehyde proceeded with yield and selectivity similar to those of the in situ procedure recently disclosed from our laboratories.[9b,d]

The behavior of nickel metallacycle **14a** described above clearly demonstrates the chemical competence of nickel metallacycles in alkylative cyclizations involving dimethylzinc, but the results tell nothing about the kinetic competence of this species in catalytic cyclizations. The catalytic cyclization of alkynyl enal **13a** with $Ni(COD)_2$/tmeda (10 mol %, 1:1) and commercial dimethylzinc (3 equiv) at 0 °C in THF (0.1 M in alkynyl enal) leads to clean production of the expected compound **19a** in a very fast reaction, with complete conversion in <5 min at 0 °C. In contrast, treatment of alkynyl enal **13a** with a stoichiometric quantity of $Ni(COD)_2$/tmeda (1:1) produces metallacycle **14a** in a much slower process, with reaction times on the order of 1−2 h being required to achieve complete conversion. Similarly, treatment of metallacycle **14a** with 3.0 equiv of dimethylzinc produces compound **19a** more slowly than catalytic cyclizations of **13a** proceed, with reaction times also

Scheme 7

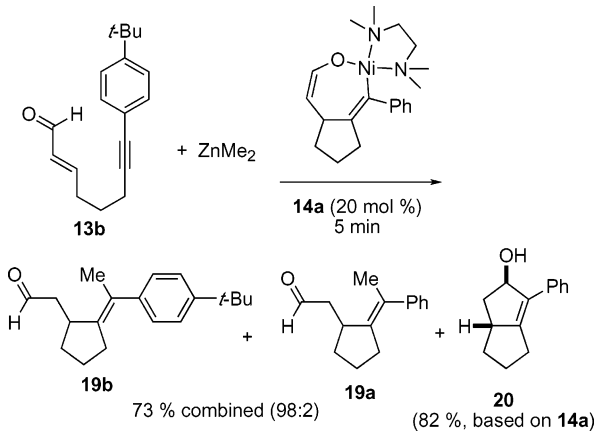

on the order of 1−2 h being required to achieve complete conversion. Thus, the conversions of both **13a** to **14a** and of **14a** to **19a** proceed too slowly to be involved in the catalytic conversion of **13a** to **19a.** Computational investigation of a model for the **13a** to **14a** conversion provided further insight into this transformation and suggested an enthalpic basis for these empirical observations (vide infra).

To rigorously establish the conclusions from these qualitative experimental observations, we examined the catalytic cyclization of **13b** with dimethylzinc using metallacycle **14a** (20 mol %) as the catalyst (Scheme 7). If metallacycle **14a** is a kinetically competent species, then a catalytic cyclization that proceeds to completion should generate a 1:5 ratio of **19a** and **19b**. However, the catalytic cyclization of **13b** with dimethylzinc using catalyst **14a** (20 mol %), in a 5 min reaction, cleanly affords products **19b** and **19a** in a 98:2 ratio. Bicycle **20**, derived from protonation of metallacycle **14a** upon workup, was isolated in 82% yield based on the original loading of metallacycle **14a**. Thus, a small portion (<10%) of the metallacycle **14a** is converted to product **19a** while generating a new nickel species that catalyzes the formation of **19b** from **13b** much more rapidly than **14a** is converted to **19a**. The majority of metallacycle **14a** persists until the reaction is quenched, which directly converts **14a** into bicycle **20**.

To provide further insight into differences between the stoichiometric transformations involving metallacycle **14a** with the overall catalytic conversion of alkynyl enal **13a** into **19a**, we examined both sets of transformations with a chiral nickel species (Scheme 8). Given the structural similarity of bis-oxazolines to tmeda and bipyridine, which stabilize the nickel metallacycles in question, we examined asymmetric transformations involving ligand **23**. Catalytic cyclizations involving $Ni(COD)_2$ and ligand **23** (1:1, 10 mol %), were quite efficient, with good yields of product **19a** being obtained in 77% yield after <5 min at room temperature. However, the reactions proceeded essentially without enantioselection, and measured ee's were <5%. Next, the stoichiometric conversion of alkynyl enal **13a** to the metallacycle upon treatment with 1.1 equiv of the 1:1 adduct of $Ni(COD)_2$ and ligand **23** was carried out, and quenching with methanol afforded bicyclooctanol **20** in 33% yield in 72:28 er. The stereochemistry-determining steps of the potentially similar catalytic production of **19a** and stoichiometric production of **20** clearly do not

Scheme 8

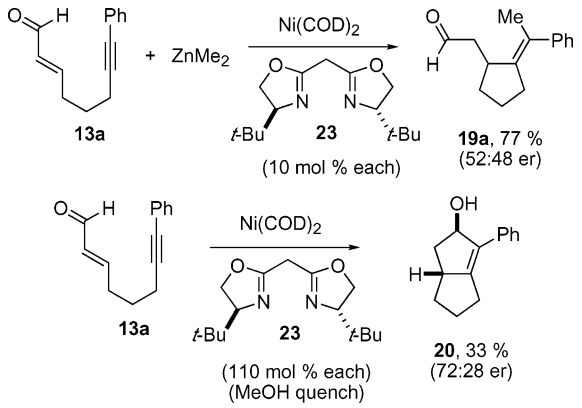

Scheme 9

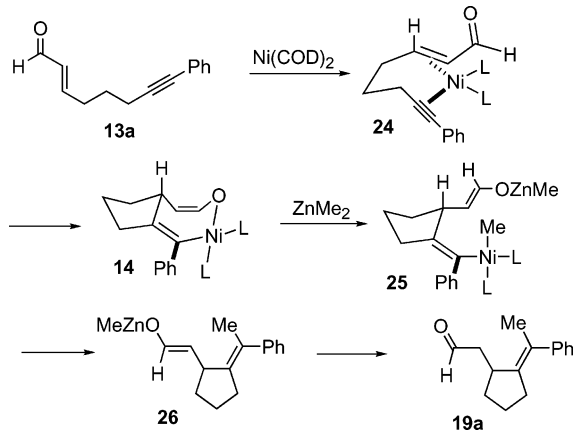

proceed in identical fashion. Interpretations of these intriguing pieces of data regarding structure, reactivity, reaction rates, and enantioselection will be discussed below.

Computational Analysis of the Organozinc Involvement

Our original interpretation of the mechanism of nickel-catalyzed cyclizations of alkynyl enals and organozincs followed well-precedented chemical steps (Scheme 9). Complexation of Ni(0) to the alkynyl enone would generate tetrahedral complex **24**. Oxidative cyclization of **24** would result in the formation of metallacycle **14** concomitant with geometric reorganization at nickel from tetrahedral to square planar as the oxidation state progresses from Ni(0) to Ni(II). Transmetalation of dimethylzinc would result in the formation of intermediate **25**, which produces the zinc enolate **26** of the observed product **19a** upon reductive elimination. In the course of these studies, complex **14** was directly isolated and characterized as the tmeda and bipyridine adducts, and two chemical models for bis π complex **24** were obtained by replacing the alkyne unit with an enone or diene.[12] However, the experiments presented above (Scheme 7 and accompanying discussion) are inconsistent with this mechanistic picture, since both the conversion of **13a** to **14a** and the conversion of **14a** to **26** are too slow to be involved in the catalytic process. In addition, the structure of the main-group organometallic was observed to have an effect on not only the regiochemistry of alkyne insertions but also the overall constitution of the products in various instances involving related reaction classes.[8e,13] It therefore became apparent that some modification of the proposed mechanism must be formulated.

Since the above experimental studies clearly demonstrated that the presence of organozincs in some way alters the reaction progression and rate in the interaction of Ni(0) with **13a**, we opted to employ a computational approach to provide insight into the precise role of the organozinc participation. Electronic structure calculations were carried out using the GAUSSIAN suite of programs.[14] All wave functions are closed-shell singlets.[15] The B3LYP density functional method and the 6-31G(d) basis set were employed.[16] Equilibrium and transition state structures were optimized using standard methods[17] and were verified by computing analytic second derivatives. Transition states were further verified by visualization of transition vectors and/or reaction path following calculations.[18]

To computationally evaluate modified mechanisms, we first evaluated our originally proposed mechanism described in Scheme 9. As a first step in our computational studies, the ground-state conformation of compound **27** possessing an ethylenediamine ligand was minimized to verify that there was an excellent agree-

(12) (a) For examples of Ni(0) complexes that possess and alkene and an alkyne unit, see: Pörschke, K.-R. *J. Am. Chem. Soc.* **1989**, *111*, 5691. (b) For an example of a nickel(II) metallacycle derived from an alkene and an alkyne unit, see ref 1d.

(13) For example, compare ref 13a−c: (a) Oblinger, E.; Montgomery, J. *J. Am. Chem. Soc.* **1997**, *119*, 9065. (b) Huang, W.-S.; Chan, J.; Jamison, T. F. *Org. Lett.* **2000**, *2*, 4221. (c) Ni, Y.; Amarasinghe, K. K. D.; Montgomery, J. *Org. Lett.* **2002**, *4*, 1743. Also see: (d) Lozanov, M.; Montgomery, J. *J. Am. Chem. Soc.* **2002**, *124*, 2106.

(14) Frisch, M. J.; Trucks, G. W.; Schlegel, H. B.; Scuseria, G. E.; Robb, M. A.; Cheeseman, J. R.; Montgomery, J. A., Jr.; Vreven, T.; Kudin, K. N.; Burant, J. C.; Millam, J. M.; Iyengar, S. S.; Tomasi, J.; Barone, V.; Mennucci, B.; Cossi, M.; Scalmani, G.; Rega, N.; Petersson, G. A.; Nakatsuji, H.; Hada, M.; Ehara, M.; Toyota, K.; Fukuda, R.; Hasegawa, J.; Ishida, M.; Nakajima, T.; Honda, Y.; Kitao, O.; Nakai, H.; Klene, M.; Li, X.; Knox, J. E.; Hratchian, H. P.; Cross, J. B.; Adamo, C.; Jaramillo, J.; Gomperts, R.; Stratmann, R. E.; Yazyev, O.; Austin, A. J.; Cammi, R.; Pomelli, C.; Ochterski, J. W.; Ayala, P. Y.; Morokuma, K.; Voth, G. A.; Salvador, P.; Dannenberg, J. J.; Zakrzewski, V. G.; Dapprich, S.; Daniels, A. D.; Strain, M. C.; Farkas, O.; Malick, D. K.; Rabuck, A. D.; Raghavachari, K.; Foresman, J. B.; Ortiz, J. V.; Cui, Q.; Baboul, A. G.; Clifford, S.; Cioslowski, J.; Stefanov, B. B.; Liu, G.; Liashenko, A.; Piskorz, P.; Komaromi, I.; Martin, R. L.; Fox, D. J.; Keith, T.; Al-Laham, M. A.; Peng, C. Y.; Nanayakkara, A.; Challacombe, M.; Gill, P. M. W.; Johnson, B.; Chen, W.; Wong, M. W.; Gonzalez, C.; Pople, J. A.; *GAUSSIAN 03*; Gaussian, Inc.: Pittsburgh, PA, 2003.

(15) All transition states were tested for SCF stability. Only **TS-30** and **TS-34** were found to have minor instabilities, and recalculating these structures as open-shell singlets lowered the energy by only 0.336 and 0.014 kcal/mol and yielded values of $\langle S^2 \rangle$ of 0.212 and 0.046, respectively. Further, the eigenvalues of the orbital rotation Hessian are −0.009 568 9 and -0.001 996 1 au, respectively. This indicates that none of the transition states have significant multireference character at this level of theory.

(16) (a) Becke, A. D. *Phys. Rev. A* **1988**, *38*, 3098. (b) Becke. A. D. *J. Chem. Phys.* **1993**, *98*, 5648. (c) Lee, T.; Yang, W. T.; Parr, R. G. *Phys. Rev. B* **1988**, *37*, 785. (d) Ditchfield, R.; Hehre, W. J.; Pople, J. A. *J. Chem. Phys.* **1971**, *54*, 724. (e) Gordon, M. S. *Chem. Phys. Lett.* **1980**, *76*, 163. (f) Hariharan, P. C.; Pople, J. A. *Theor. Chim. Acta* **1973**, *28*, 213. (g) Hariharan, P. C.; Pople, J. A. *Mol. Phys.* **1974**, *27*, 209. (h) Hehre, W. J.; Ditchfield, R.; Pople, J. A. *J. Chem. Phys.* **1972**, *56*, 225.

(17) (a) Schlegel, H. B. *J. Comput. Chem.* **1982**, *3*, 214. (b) Peng, C.; Schlegel, H. B. *Isr. J. Chem.* **1993**, *33*, 449. (c) Peng, C.; Ayala, P. Y.; Schlegel, H. B.; Frisch, M. J. *J. Comput. Chem.* **1996**, *17*, 49.

(18) (a) Gonzalez, C.; Schlegel, H. B. *J. Chem. Phys.* **1989**, *90*, 2154. (b) Gonzalez, C.; Schlegel, H. B. *J. Phys. Chem.* **1990**, *94*, 5523. (c) Hratchian, H. P.; Schlegel, H. B. *J. Phys. Chem. A* **2002**, *106*, 165. (d) Hratchian, H. P.; Schlegel, H. B. *J. Chem. Phys.* **2004**, *120*, 9918−9924. (e) Hratchian, H. P.; Schlegel, H. B. *J. Chem. Theor. Comput.*, in press.

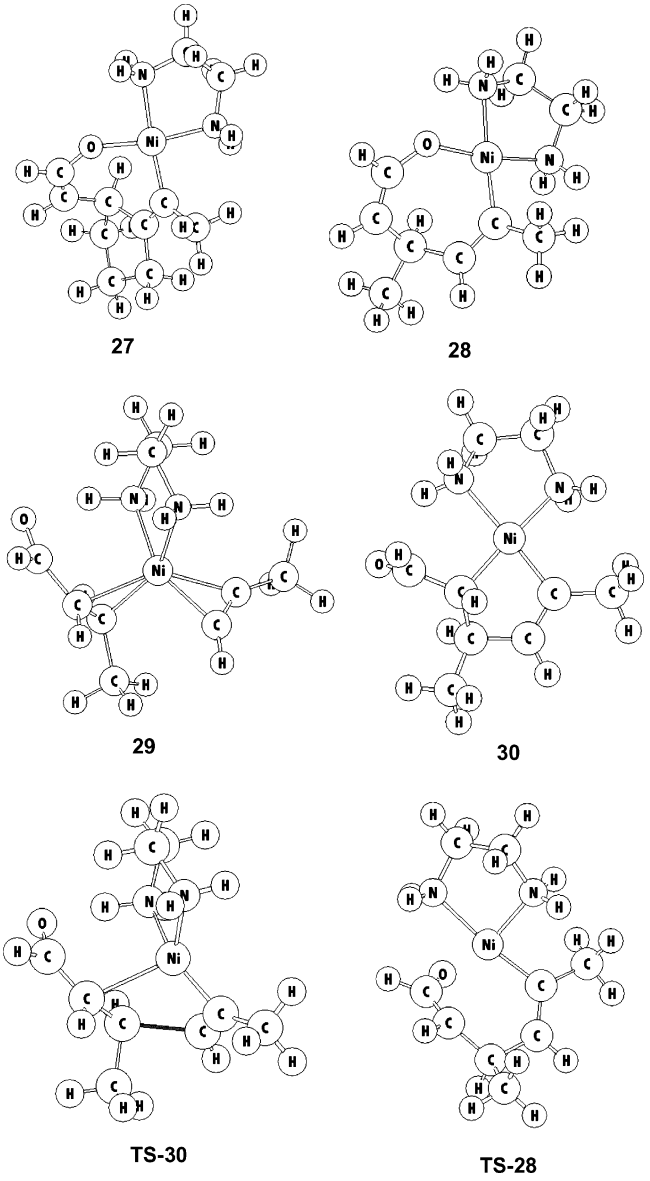

Figure 5. Optimized geometries for **27** and minima and transition states involved in the formation of **28** from **29**.

ment between the solid-state structure of **14a**, as determined by X-ray crystallography (Figure 1), and the computationally derived conformation of structure **27** (Figure 5). The conformation of the simpler metallacycle **28** (Figure 5) derived from crotonaldehyde and propyne was then determined computationally, and all three structures **14a**, **27**, and **28** were found to provide good agreement in the structural characteristics within the metallacycle framework (Table 1). The crystallographically characterized bis-enone π complex structure **16** (Figure 3) was then modified to include the relevant enal and alkyne functionalities and the ethylenediamine ligand motif, and minimization of the energy of that structure then provided the ground-state complex **29** that would lead to metallacycle **28** upon oxidative cyclization (Figure 5).

Comparison of the relative energies of the two structures **28** and **29** revealed that metallacycle **28** was more stable by 13.9 kcal/mol (Figure 6). In searching for a transition state for this conversion, intermediate **30** was found on the reaction path that possessed a five-membered metallacycle with an η^1 *C*-enolate structural

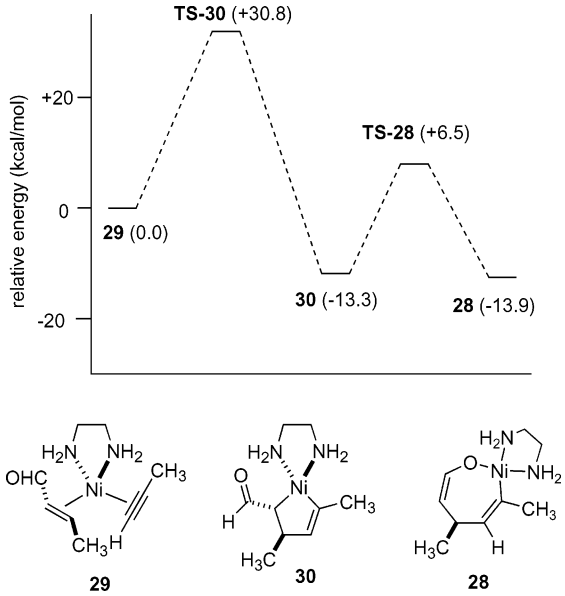

Figure 6. Energy changes of the **29** to **28** reaction at the B3LYP/6-31G(d) level. Values in parentheses are energies relative to the reactant in kcal/mol.

Table 1. Selected Bond Lengths (Å) and Angles (deg) of 14a, 27, and 28

	14a	27	28
Ni−O	1.852(6)	1.8138	1.8157
Ni−C	1.897(7)	1.8742	1.8744
Ni−N_1	1.982(6)	1.9314	1.9301
Ni−N_2	2.077(7)	2.0303	2.0254
O−Ni−C	91.3(3)	98.10	97.85
C−Ni−N_1	94.3(3)	91.79	92.09
N_1−Ni−N_2	85.6(3)	84.61	84.81
N_2−Ni−O	88.9(3)	85.51	85.28

motif. This intermediate was 13.3 kcal/mol lower in energy than the starting π complex **29** and, thus, slightly higher in energy (by 0.6 kcal/mol) than the rearranged *O*-enolate **28**. The transition-state structure and energies for the conversion of **29** to **30** and for **30** to **28** were determined. The barrier for the oxidative cyclization (**29** to **30**) was 30.8 kcal/mol, and the barrier for the *C*-enolate to *O*-enolate tautomerization (**30** to **28**) was 19.8 kcal/mol.[19] As expected, the transition state for the **29** to **30** conversion involves formation of the C−C bond and geometric reorganization of the transition-metal center from tetrahedral to square planar. The geometry at nickel of **TS-30** is slightly distorted tetrahedral. A stability test of the closed-shell singlet wave function indicated a slight RHF/UHF instability.[15] This suggests that the oxidation of Ni(0) in the **29** to **30** conversion occurs early in the reaction and occurs more quickly than the geometric rearrangement. The transition state for the **30** to **28** conversion adopts an enolate binding motif that resembles an η^3-enolate structure as the tautomerization and ring expansion occurs. Most features of this overall conversion are consistent with expectations, but the energy barrier for the initial oxidative cyclization is very high for an efficient catalytic process. This high barrier for oxidative cyclization is consistent with the experimental observation that the

(19) For a recent discussion of C- and O-tautomers of nickel enolates, see: Campora, J.; Maya, C. M.; Palma, P.; Carmona, E.; Gutiérrez-Puebla, E.; Ruiz, C. *J. Am. Chem. Soc.* **2003**, *125*, 1482.

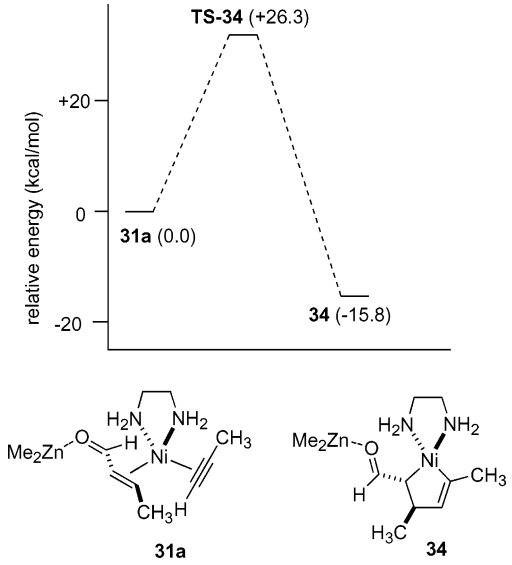

Figure 7. Energy changes of the **31a** to **34** reaction at the B3LYP/6-31G(d) level. Values in parentheses are energies relative to the reactant in kcal/mol.

Chart 1

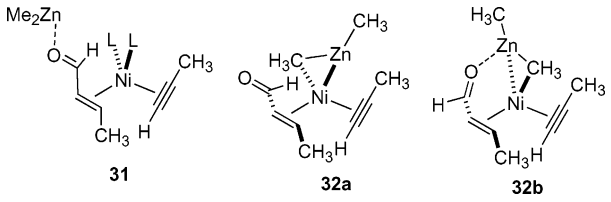

stoichiometric oxidative cyclization proceeds slowly in the absence of organozinc. The basic features of the proposed mechanism may be correct, but if metallacycle formation is involved in the process, then the organozinc must be involved in a rate acceleration of the metallacycle-forming process.

We consider three roles to be most likely for the organozinc: Lewis acidic activation of the enal carbonyl (**31**), Lewis basic activation of a Ni(0) species via three-center−two-electron bridging of the zinc−methyl bond with nickel (**32a**), or a combination of the two effects (**32b**) (Chart 1).[20]

Lewis acid activation of the enal carbonyl was first considered (Figures 7 and 8). In our computational analysis, Lewis acidic activation of the carbonyl oxygen results in the *C*-enolate metallacycle **34**, which is formed with an activation barrier of 26.3 kcal/mol. Similar to the **29** to **30** conversion, the oxidation of Ni(0) occurs more rapidly than the geometric rearrangement of the transition-metal center in the **31a** to **34** conversion.[15] The five-membered *C*-enolate metallacycle **34** is more stable than the ground-state π complex **31a** by 15.8 kcal/mol. An absolute comparison of the ground-state energies of **29** and **31a** or of **30** and **34** is not meaningful, since the structures are not constitutional isomers. However, the relatively large $\Delta H^{\ddagger}$ value for the organozinc-promoted pathway suggests that a simple Lewis acidic interaction of the organozinc reagent does not satisfactorily explain the efficient catalysis observed.

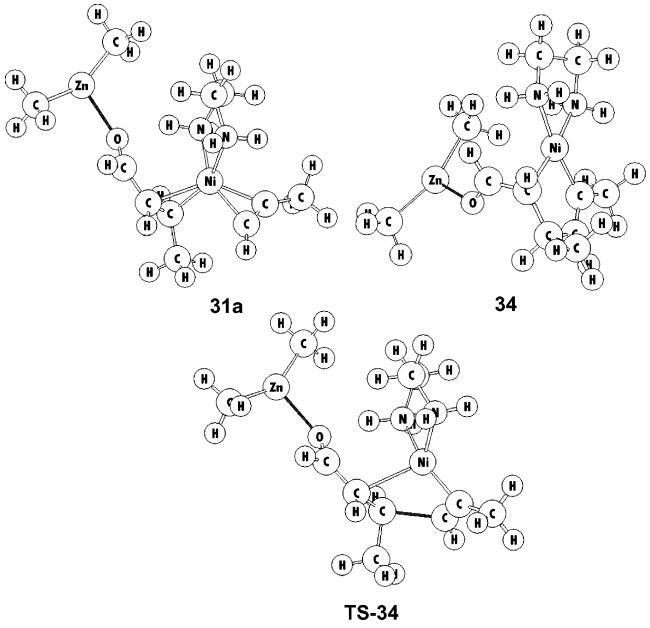

Figure 8. Optimized geometries for the structures involved in the formation of **34** from **31a**.

Chart 2. Crystallographically Characterized Adducts (Pörschke and Wilke)

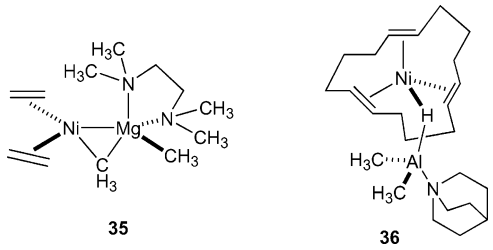

A Lewis basic interaction of the organozinc with Ni(0) was considered next. In searching for examples of various metal alkyls and metal hydrides that interact with Ni(0) complexes, work from Pörschke and Wilke emerged as the most relevant structures that directly document such an interaction (Chart 2).[1a,21] Studies from those laboratories elegantly demonstrated that Ni(0) serves as a Lewis acid in the presence of metal alkyls and metal hydrides. In particular, two relevant crystal structures have been reported: one (**35**) documents the direct coordination of tmeda-ligated dimethylmagnesium with a Ni(0) bis(ethylene) complex, and the second (**36**) documents the direct coordination of quinuclidine-ligated dimethylaluminum hydride with a Ni(0) cyclododecatriene complex. We envision that these coordination modes may serve as excellent models for the manner in which organozincs, organosilanes, and other reducing agents may interact with the Ni(0) π complexes that are relevant to the catalytic processes developed in our laboratory. Such an interaction could explain the role of the organozinc in controlling the rate,

(20) For discussion of interactions of metal hydrides or metal alkyls with nickel in catalytic processes, see: (a) Lautens, M.; Ma, S.; Chui, P. *J. Am. Chem. Soc.* **1997**, *119*, 6478. (b) Lautens, M.; Rovis, T. *J. Am. Chem. Soc.* **1997**, *119*, 11090. (c) Terao, J.; Oda, A.; Ikumi, A.; Nakamura, A.; Kuniyasu, H.; Kambe, N. *Angew. Chem., Int. Ed.* **2003**, *42*, 3412. (d) Subburaj, K.; Montgomery, J. *J. Am. Chem. Soc.* **2003**, *125*, 11210. (e) Mahandru, G. M.; Liu, G.; Montgomery, J. *J. Am. Chem. Soc.* **2004**, *126*, 3698.

(21) (a) Kaschube, W.; Pörschke, K.-R.; Angermund, K.; Krüger, C.; Wilke, G. *Chem. Ber.* **1988**, *121*, 1921. (b) Pörschke, K.-R.; Kleimann, W.; Tsay, Y.-H.; Krüger, C.; Wilke, G. *Chem. Ber.* **1990**, *123*, 1267. (c) Jonas, K.; Pörschke, K.-R.; Krüger, C.; Tsay, Y.-H. *Angew. Chem., Int. Ed. Engl.* **1976**, *15*, 621. (d) Pörschke, K.-R.; Jonas, K.; Wilke, G. *Chem. Ber.* **1988**, *121*, 1913.

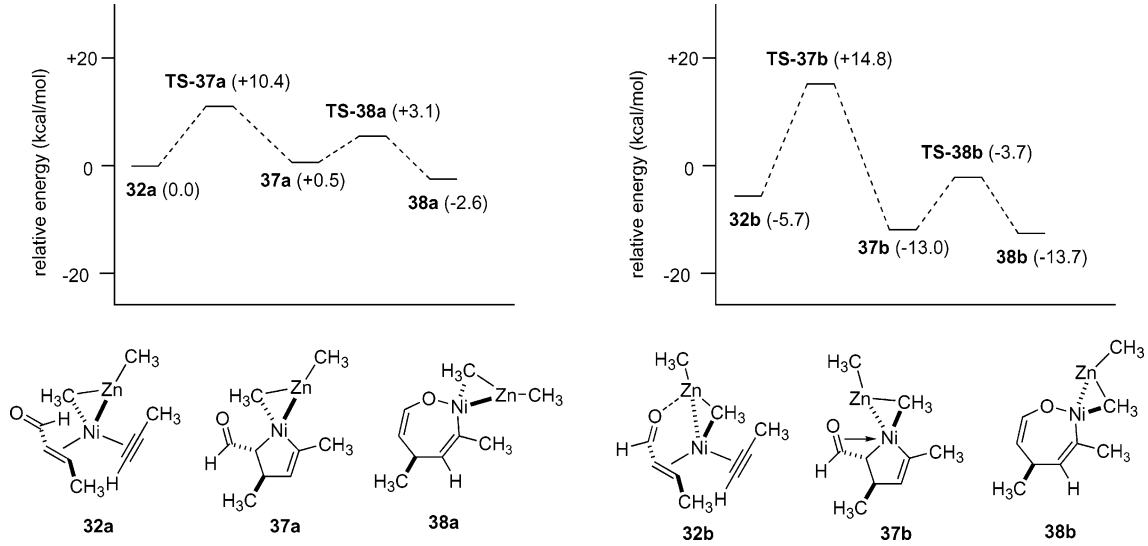

Figure 9. Energy changes of the **32a** to **38a** reaction and the **32b** to **38b** reaction at the B3LYP/6-31G(d) level. Values in parentheses are energies relative to **32a** in kcal/mol.

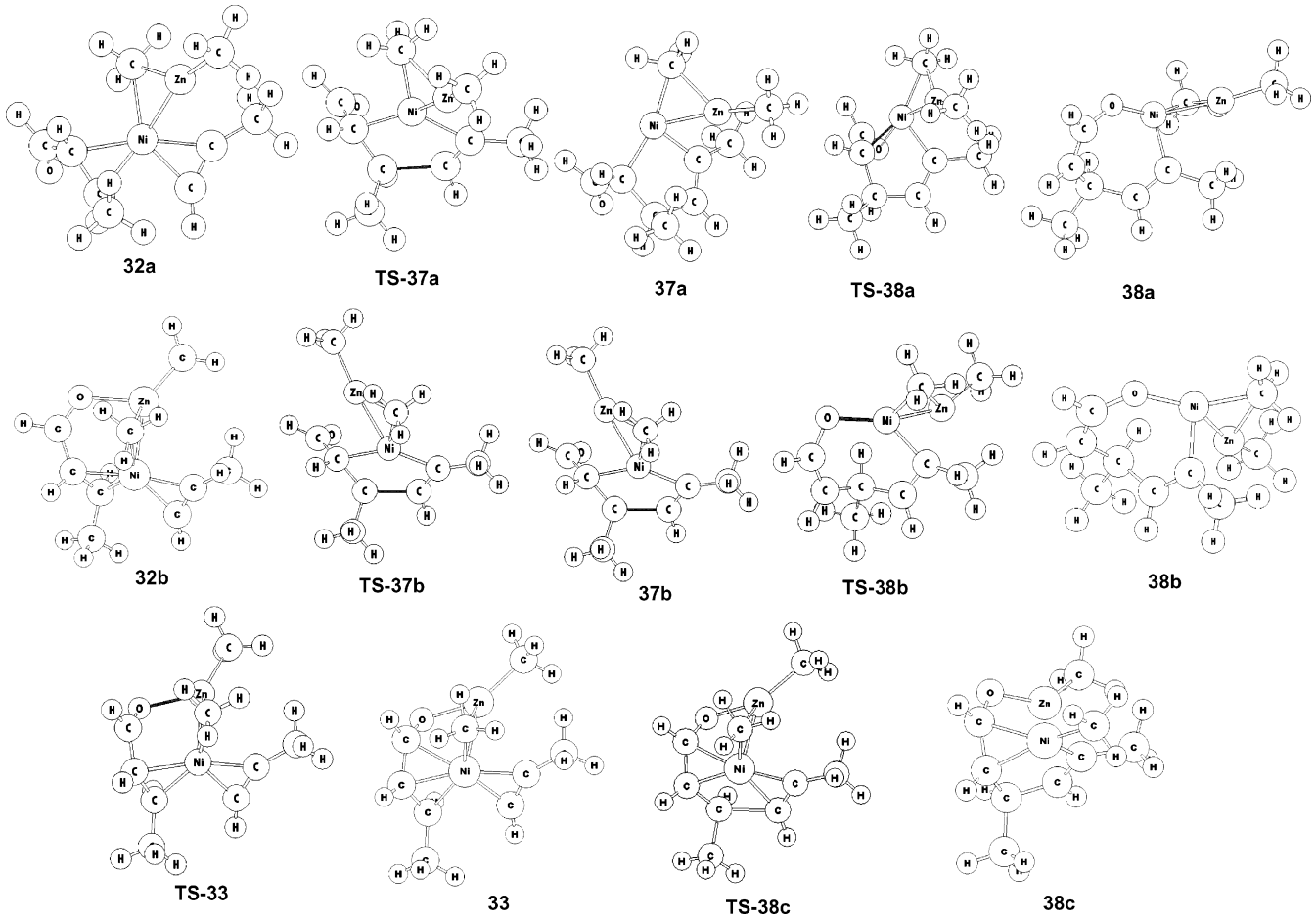

Figure 10. Optimized geometries for the structures involved in the formation of **38a** from **32a**, **38b** from **32b**, and **38c** from **32b**.

regiochemistry, and constitution of products obtained in catalytic cyclizations and additions.

Lewis basic activation of a Ni(0) species via three-center−two-electron bridging of the zinc−methyl bond with nickel can proceed via the two isomeric ground-state adducts **32a** and **32b** (Figures 9 and 10), with isomer **32b** possessing an additional stabilizing Zn−O interaction not possible in **32a**. Adduct **32a** is the least stable of these by 5.7 kcal/mol, but the resulting activation barrier for the oxidative cyclization of **32a** is quite low ($\Delta H^{\ddagger} = 10.4$ kcal/mol). In contrast, adduct **32b**, whose ground-state energy is 5.7 kcal/mol lower than that of adduct **32a**, undergoes oxidative cyclization to a metallacycle with a higher barrier of $\Delta H^{\ddagger} = 20.5$ kcal/mol. Thus, the energy of **TS-37a** is lower than that of **TS-37b** by 4.4 kcal/mol.

Most interestingly, an alternate rearrangement pathway that involves **32b** provides the lowest barrier for

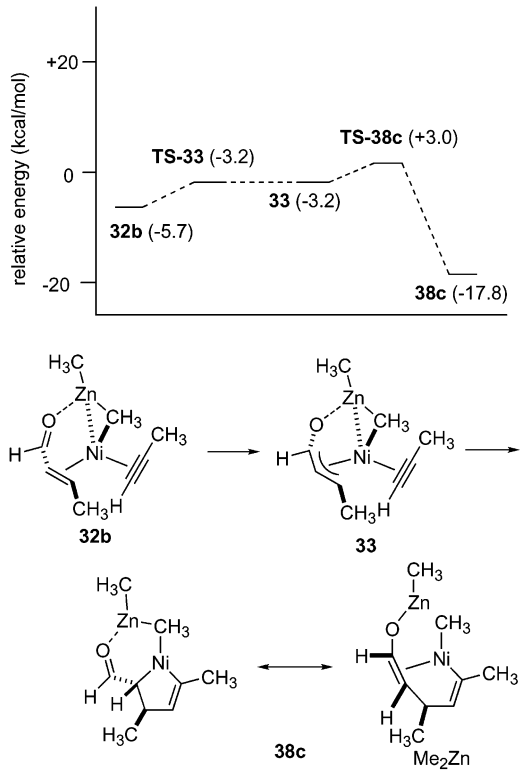

Figure 11. Energy changes of the **32b** to **38c** reaction at the B3LYP/6-31G(d) level. Values in parentheses are energies relative to **32a** in kcal/mol.

the overall transformation (Figures 10 and 11). Starting from adduct **32b**, a formal oxidative addition of Ni(0) to the Lewis acid activated enone proceeds with a very low barrier of 2.5 kcal/mol to produce the bicyclic π-allyl intermediate **33**,[22] which itself is 2.5 kcal/mol less stable than adduct **32b**. In contrast to the 20.5 kcal/mol barrier observed for the direct oxidative cyclization of **32b**, adduct **33** undergoes cyclization to metallacycle **38c** with a barrier of only 6.2 kcal/mol, making the overall barrier for the conversion of **32b** to **33** to metallacycle **38c** significantly lower than any other pathway examined. The conversion of **33** to **38c** is accompanied by a weakening of the bridging zinc−carbon and zinc−nickel interactions. Therefore, structure **38c** is best represented as a hybrid of the two resonance extremes depicted (Figure 11).

The three-membered ring observed in the characterized $MgMe_2$ adduct of Ni^0 and the computationally predicted $ZnMe_2$ adducts of Ni^0 involve very unusual interactions. We therefore employed the natural bond orbital (NBO) analysis of Weinhold and co-workers to examine the bonding in structures **32a** and **32b**.[23] We have specifically made use of the second-order perturbation analysis of the canonical NBOs to determine the stabilization energies of NBOs due to interactions between fragment orbitals. Each ligand on the nickel has been defined as a separate fragment, and the Ni atom is defined as a fourth fragment. Not surprisingly, the key interaction of the bridging alkyl in both **32a** and

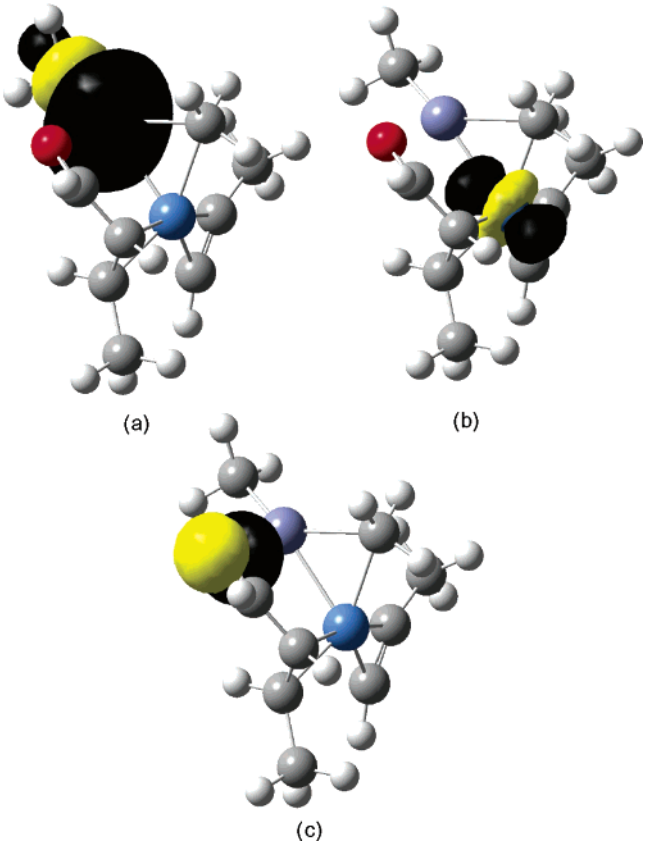

Figure 12. Key orbital interactions in **32b**: (a) unoccupied Zn−C σ* orbital; (b) occupied Ni d_{z^2} orbital; (c) oxygen lone-pair orbital involved in donation to Zn-centered orbital.

32b involves σ-donation of Zn−C bonding electrons to the unoccupied nickel 4s orbital.[24] However, an unusual bonding interaction predicted by theory is the significant back-bonding of the filled Ni $3d_{z^2}$ orbital with the σ* orbital of the nonbridging Zn−C bond (Figure 12). It is this latter interaction that causes the short interatomic distance between Ni and Zn (2.3 Å).[25] For both **32a** and **32b**, the stabilization energies arising from these two interactions between the Me_2Zn and Ni fragments are roughly equivalent (within 2.5 kcal/mol). **32b** is further stabilized by an interaction between the enone and Me_2Zn fragments. This interaction, which is not present in **32a**, is characterized by donation from a lone-pair orbital on O to the same Zn−nonbridging Me σ* orbital involved in back-donation from Ni.

(22) (a) Johnson, J. R.; Tully, P. S.; Mackenzie, P. B.; Sabat, M. *J. Am. Chem. Soc.* **1991**, *113*, 6172. (b) Grisso, B. A.; Johnson, J. R.; Mackenzie, P. B. *J. Am. Chem. Soc.* **1992**, *114*, 5160. (c) Ogoshi, S.; Yoshida, T.; Nishida, T.; Morita, M.; Kurosawa, H. *J. Am. Chem. Soc.* **2001**, *123*, 1944.

(23) (a) Carpenter, J. E.; Weinhold, F. *J. Mol. Struct. (THEOCHEM)* **1988**, *46*, 41. (b) Carpenter, J. E. Ph.D. Thesis, University of Wisconsin, 1987. (c) Foster, J. P.; Weinhold, F. *J. Am. Chem. Soc.* **1980**, *102*, 7211. (d) Reed, A. E.; Weinhold, F. *J. Chem. Phys.* **1983**, *78*, 4066. (e) Reed, A. E.; Weinhold, F. *J. Chem. Phys.* **1985**, *83*, 1736. (f) Reed, A. E.; Weinstock, R. B.; Weinhold, F. *J. Chem. Phys.* **1985**, *83*, 735. (g) Reed, A. E.; Curtiss, L. A.; Weinhold, F. *Chem. Rev.* **1988**, *88*, 899. (h) Weinhold, F.; Carpenter, J. E. *The Structure of Small Molecules and Ions*, Plenum: Amsterdam, 1988, p 227.

(24) For an analysis of molecular orbitals in dimethylzinc, see: Mori, S.; Hirai, A.; Nakamura, M.; Nakamura, E. *Tetrahedron* **2000**, *56*, 2805.

(25) (a) For an example of a Zn−Ni bond, see: Budzelaar, P. H. M.; Boersma, J.; van der Kerk, G. J. M. *Organometallics* **1985**, *4*, 680. (b) For an example of a Pt−Cd bond that involves donation from a filled d_{z^2} orbital to a vacant orbital on Cd, see: Yamaguchi, T.; Yamazaki, F.; Ito, T. *J. Am. Chem. Soc.* **1999**, *121*, 7405. (c) For a general discussion of transition-metal/main-group-metal bonding, see: Frenking, G. F. *J. Organomet. Chem.* **2001**, *635*, 9. (d) For a general discussion of the influence of back-bonding interactions on d^{10} metal reactivity, see: Stahl, S. S.; Thorman, J. L.; de Silva, N.; Guzei, I. A.; Clark, R. W. *J. Am. Chem. Soc.* **2003**, *125*, 12.

Given these bonding characteristics, the question then arises regarding the origin of differences among **TS-37a**, **TS-37b**, and **TS-33**. Our analysis suggests that **TS-37a** is lower in energy than **TS-37b** because the weak zinc−oxygen interaction present in **32b** is broken in **TS-37b** as the nickel enolate adopts an η^3 interaction. However, the weak zinc−oxygen interaction of **32b** is further strengthened in **TS-33**, and that favorable interaction leads to the overall low barrier for the **32b** to **38c** conversion.

Discussion and Implications

This mechanism involving a dual Lewis basic/Lewis acidic role of the organozinc (Figure 11) possesses a number of attractive features. It involves the core idea of metallacycle involvement, which explains many of the synthetic results, and it is consistent with the qualitative kinetic observations described above. The important experiment described in Scheme 7, which demonstrated that metallacycle **14a** is not kinetically competent in the catalytic conversion of alkynyl enal **13b** to product **19b**, may be rationalized by a mechanism that involves formation of an active Ni(0)/$ZnMe_2$ adduct. The trace quantity of product **19a** obtained is derived from conversion of a small portion of metallacycle **14a** into product **19a**. Interaction of dimethylzinc with the nickel(0) species generated by production of compound **19a** then generates a more active catalyst that rapidly converts substrate **13b** into product **19b**, perhaps by the mechanism depicted in Figure 11. The majority of metallacycle **14a** is unchanged during the short reaction time (5 min) and is converted upon workup into bicycle **20**.

Furthermore, as the rates of many metal-catalyzed cross-couplings are restricted by a rate-determining transmetalation event,[26] the proposed prior coordination of the organozinc avoids this potential complexity, since a unimolecular rearrangement is required for metallacycle **38c** to be converted to product. Although the final stages of the overall catalytic process were not modeled in this study, it is interesting to note that intermediate **38c** is ideally positioned to undergo the required carbon−carbon bond-forming reductive elimination that would allow product formation. Alternatively, structure **34**, which is formed by the Lewis acidic role of the organozinc (Figures 7 and 8), would likely require a potentially high barrier ligand dissociation during the Zn to Ni transmetalation event. Furthermore, we reiterate that $Ni(COD)_2$ itself in the absence of diamines is the typical formulation for efficient catalytic cyclizations, and the diamine formulations were investigated simply to allow study of the kinetic competence of the tmeda metallacycle that was isolated. Thus, an overall mechanism that incorporates the experimental observations reported herein and that embodies the computationally predicted interactions of dimethylzinc and Ni(0) may be formulated as shown (Scheme 10).

The divergent enantioselectivity results (Scheme 8) may also be readily rationalized by this mechanism. The [3 + 2] reductive cycloaddition to form product **20** in

Scheme 10

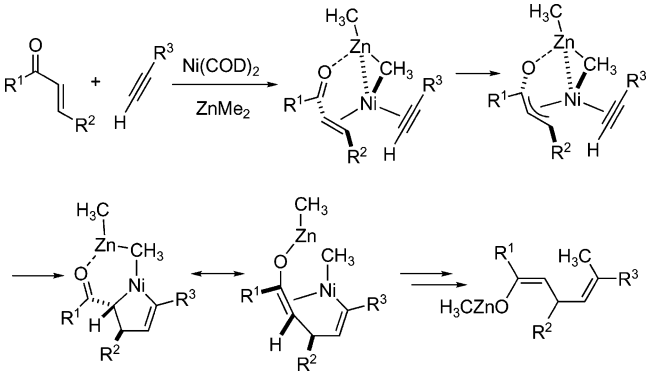

the absence of organozincs likely proceeds with bidentate coordination of the bis(oxazoline) in a stereochemistry-determining oxidative cyclization. Methanol quenching results in liberation of the bicyclooctenol product **20** with conservation of enantioselectivity. If the organozinc-mediated cyclization to give product **19a** proceeds via the same metallacycle, then the enantioselectivities for the production of compounds **19a** and **20** would likely be similar. However, if the organozinc serves to sequester the bis(oxazoline), then an equilibrium concentration of a more reactive achiral catalyst, which involves an association of nickel with $ZnMe_2$ (as depicted in Figure 11 and Scheme 10), rather than with the bis(oxazoline), could be responsible for the production of racemic **19d**. Another potential explanation is that **19a** is produced from a metallacycle generated under kinetic control with poor enantioselection, whereas **20** is produced from the metallacycle generated stoichiometrically under thermodynamic conditions with better (72:28) enantioselection,[27] although we favor the former explanation. Indeed, the ground-state interactions depicted in the crystallographically characterized adduct of dimethylmagnesium, tmeda, and Ni(0) from Pörschke and Wilke (Chart 2) depicts exactly this type of interaction wherein direct association of Ni(0) with the diamine is clearly not involved.

We believe that the above mechanistic suggestions could have implications in many classes of related transformations. For instance, one previously unexplained observation from our group and from Jamison is the diverging selectivities for ethyl vs hydrogen atom incorporation in nickel-catalyzed cyclizations and couplings involving either diethylzinc or triethylborane.[8g,13] If the extent of bridging between nickel and either zinc or boron is significantly different, then significant differences in the relative rates of processes involving selectivity-determining reductive elimination and β-hydride elimination from a bridged ethyl species would not be at all surprising. Another unexplained feature of aldehyde−alkyne couplings from our earlier work is the regiochemical reversal of alkyne insertion in intermolecular processes involving either alkenylzirconocenes or alkylzincs as the reducing agent.[13] If the oxidative

(26) (a) Amatore, C.; Bahsoun, A. A.; Jutand, A.; Meyer, G.; Ntepe, A. N.; Ricard, L. *J. Am. Chem. Soc.* **2003**, *125*, 4212. (b) Louie, J.; Hartwig, J. F. *J. Am. Chem. Soc.* **1995**, *117*, 11598. (c) Farina, V.; Krishnan, B. *J. Am. Chem. Soc.* **1991**, *113*, 9585.

(27) We are unaware of an exact precedent for this possibility. However, very different kinetic and thermodynamic cis/trans selectivities in the zirconocene-catalyzed cyclomagnesiation of dienes is well established: (a) Knight, K. S.; Wang, D.; Waymouth, R. M.; Ziller, J. *J. Am. Chem. Soc.* **1994**, *116*, 1845. (b) Taber, D. F.; Louey, J. P.; Wang, Y.; Nugent, W. A.; Dixon, D. A.; Harlow, R. L. *J. Am. Chem. Soc.* **1994**, *116*, 9457.

cyclization involves a Ni(0) species complexed to the organozinc or alkenylzirconium, then the dramatically different steric properties of these two types of reagents would be expected to play an important role in alkyne regioselection. We do not mean to imply that ligand sequestration routinely occurs in reactions of this general class. Important ligand effects have been documented, and various enantioselective chiral ligand-based transformations have been reported.[8g,28] However, there may be instances where organozincs can sequester certain ligand classes, or their interaction with Ni(0) catalysts may occur in concert with more classical metal−ligand interactions such as phosphine−nickel dative bonding.

In an even broader context, we suggest that the interaction of main-group transmetalating agents and late-metal catalysts may play a role in the oxidative addition step of many classes of cross-coupling processes. Elegant studies from Amatore and Jutand have clearly demonstrated that chloride association with Pd(0) generates an active catalyst in oxidative addition processes.[29] A similar interaction of transmetalating agents with late-metal cross-coupling catalysts via the interaction modes described herein may, in some instances, be involved in catalytic mechanisms as well.[30]

Acknowledgment. J.M. thanks the National Science Foundation (Grant No. CHE-0405800), Johnson and Johnson (Focused Giving Grant), the Camille and Henry Dreyfus Foundation (Teacher Scholar Award), and the American Chemical Society (Arthur C. Cope Scholar Award) for support, H.B.S. thanks the National Science Foundation (Grant No. CHE 0131157) and the National Computational Science Alliance (Grant No. CHE980042N) for support, V.M.G.-G. thanks the CONACYT-México for a postdoctoral fellowship, and H.P.H. thanks the Institute for Scientific Computing at Wayne State University for support provided by an NSF-IGERT fellowship.

Supporting Information Available: Text giving full experimental details, figures giving ^{1}H NMR spectra of all new compounds, and tables giving X-ray crystallographic data and SCF energies and gas-phase Cartesian coordinates for the structures studied computationally; crystallographic data are also given as CIF files. This material is available free of charge via the Internet at http://pubs.acs.org.

OM049471A

(28) (a) Ikeda, S.; Cui, D.-M.; Sato, Y. *J. Am. Chem. Soc.* **1999**, *121*, 4712. (b) Sato, Y.; Saito, N.; Mori, M. *J. Am. Chem. Soc.* **2000**, *122*, 2371. (c) Montgomery, J.; Savchenko, A. V. *J. Am. Chem. Soc.* **1996**, *118*, 2099.

(29) (a) Amatore, C.; Azzabi, M.; Jutand, A. *J. Am. Chem. Soc.* **1991**, *113*, 8375. (b) Amatore, C.; Jutand, A.; Suarez, A. *J. Am. Chem. Soc.* **1993**, *115*, 9531. (c) Amatore, C.; Jutand, A. *Acc. Chem. Res.* **2000**, *33*, 314. (d) Amatore, C.; Carré, E.; Jutand, A.; Tanaka, H.; Ren, Q.; Torii, S. *Chem. Eur. J.* **1996**, *2*, 957.

(30) Although we believe that reaction acceleration by coordination of a transmetalation agent prior to oxidative addition should be considered in some cross-coupling processes, it is clearly not a general phenomenon. For instance, prior coordination of an alkenylstannane to $Pd(AsPh_3)_2$ in Stille couplings was demonstrated to have a decelerating effect: Amatore, C.; Bahsoun, A. A.; Jutand, A.; Meyer, G.; Ntepe, A. N.; Ricard, L. *J. Am. Chem. Soc.* **2003**, *125*, 4212.

2004, Volume 23

Hrant P. Hratchian, Sanjoy K. Chowdhury, Victor M. Gutierrez-Garcia, Kande K. D. Amarasinghe, Mary Jane Heeg, H. Bernhard Schlegel, and John Montgomery: Combined Experimental and Computational Investigation of the Mechanism of Nickel-Catalyzed Three-Component Addition Processes

Pages 4641−4642. Structures **30** and **34** were incorrectly drawn in Figures 6 and 7. The corresponding computationally derived depictions in Figures 5 and 8 are correctly shown. The corrected representations are given below.

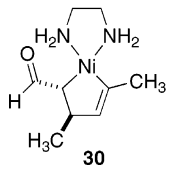

30

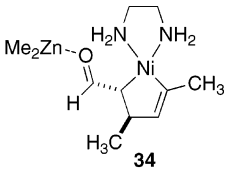

34

OM0492799

10.1021/om0492799 CCC: $27.50
Publication on Web 00/00/0000 PAGE EST: 0.3